Cancer Letters 461 (2019) 31–43

Contents lists available at ScienceDirect

Cancer Letters

journal homepage: www.elsevier.com/locate/canlet

Original Articles

Synthetic lethality of combined AT-101 with idarubicin in acute myeloid leukemia via blockade of DNA repair and activation of intrinsic apoptotic pathway

Qianying Yang[a,b,1], Kai Chen[c,d,1], Leisi Zhang[e,1], Liying Feng[a], Guofeng Fu[b], Shan Jiang[b], Silei Bi[a], Chunjie Lin[b], Yong Zhou[a], Haijun Zhao[a], Xiao Lei Chen[b], Guo Fu[b,**], Bing Xu[a,*]

[a] Department of Hematology, The First Affiliated Hospital of Xiamen University, Xiamen, Fujian, 361003, China
[b] State Key Laboratory of Cellular Stress Biology, Innovation Center for Cell Signaling Network, School of Life Sciences, Xiamen University, Xiamen, Fujian, 361102, China
[c] The First People's Hospital of Foshan (The Affiliated Foshan Hospital of Sun Yat-sen University), Foshan, Guangdong, 528000, China
[d] Department of Hematology, Nanfang Hospital, Southern Medical University, Guangzhou, Guangdong, 510515, China
[e] Department of Hematology, The First Affiliated Hospital of Soochow University, Suzhou, Jiangsu, 215000, China

ARTICLE INFO

Keywords:
AT-101
Idarubicin
Acute myeloid leukemia
DNA damage repair response
Intrinsic apoptotic pathway

ABSTRACT

Leukemia stem cells (LSCs) are deemed to the mainspring for treatment failure in acute myeloid leukemia (AML). Conventional chemotherapeutic drugs fail to eradicate leukemia stem cells, which becomes the root of drug resistance and disease recurrence. Hence, new therapeutic strategies targeting LSCs are supposed to be critical for patients with AML. Here we report that combination of Bcl-2 inhibitor AT-101 and chemotherapeutic drug idarubicin (IDA) results in synergistic lethality in $CD34^+CD38^-$ leukemia stem-like cells sorted from KG-1α and Kasumi-1 AML cell lines and primary $CD34^+$ AML cells *in vitro* while sparing the normal counterparts. In addition, combinatorial treatment also significantly inhibits the growth of patient-derived xenograft (PDX) mouse models generated from $FLT3\text{-}ITD^{mut}$ AML patient *in vivo*. Mechanistically, the synergistic effects of AT-101 with IDA to induce cell death are closely associated with blockage of DNA damage repair and thus activates the intrinsic apoptotic pathway. In summary, these findings suggest that combinatorial therapy with AT-101 and IDA selectively eliminates leukemia stem-like cells both *in vitro* and *in vivo*, representing a potent and alternative salvage therapy for the treatment of relapsed and refractory patients with AML.

1. Introduction

Acute myeloid leukemia is a malignant disease derived from bone marrow hematopoietic stem cells [1,2]. Despite tremendous progress in the treatment of AML, there still has a large proportion of patients died from recurrence of disease due to the existence of leukemia stem cells (LSCs) [3,4]. LSCs, like hematopoietic stem cell, are characterized by self-renewal, unlimited proliferation, and multi-differentiation potential. They are relatively quiescent and highly resistant to chemotherapy, which contribute to the dismal clinical outcomes for patients with AML [5]. Therefore, new therapeutic strategies targeting LSCs are urgently needed in order to prolong the long-term disease-free survival of patients with AML.

In general, LSCs only account for a small percentage in leukemia cells. They are phenotypically $CD34^+CD38^-$ as this fraction can develop human AML in immunodeficient mice [6–8]. KG-1α and Kasumi-1 cell lines, which are both characterized by a high percentage of cells with the stem cell-like phenotype $CD34^+CD38^-$, and therefore provide powerful tools for studies of LSCs as substitute models [9,10].

Bcl-2 and related proteins are key regulators of apoptosis [11–13], which are frequently expressed in cancer stem cells of solid tumors and hematologic malignancies. Overexpression of Bcl-2 is associated with chemotherapy resistance, resulting in dismal clinical response rates and shortened survivals [14]. AT-101, a BH3 mimetic pan-Bcl-2 inhibitor, is capable of binding Bcl-2, Bcl-xL, and Mcl-1, attenuating their anti-apoptotic efficacy. Reportedly, AT-101 exerted great anti-tumor

* Corresponding author. Department of Hematology, the First Affiliated Hospital of Xiamen University and Institute of Hematology, Medical College of Xiamen University, No.55, Zhenhai Road, Xiamen, Fujian, 361003, China.
** Corresponding author. School of Life Sciences (Huang Chaoyang Building, F114), Xiamen University, South Xiang'an Road, Xiang'an District, Xiamen, Fujian, 361102, China.
E-mail addresses: guofu@xmu.edu.cn (G. Fu), xubingzhangjian@126.com (B. Xu).
[1] These authors contributed equally.

https://doi.org/10.1016/j.canlet.2019.07.003
Received 20 April 2019; Received in revised form 28 June 2019; Accepted 5 July 2019

property in multiple cancers, such as B-cell lymphoma [15], chronic lymphocytic leukemia [16], prostate cancer [17,18], ovarian cancer [19,20], lung cancer [21] and so on. In our previous study, we had demonstrated that AT-101 could target leukemia stem-like cells for cytotoxicity, meanwhile largely spared normal hematopoietic cells [22]. However, given the molecular complexity of AML, it is highly unlikely that AML could be cured with monotherapy. Therefore, we test whether combination of already established effective drug such as IDA (a topoisomerase II inhibitor) with AT-101 can enhance or improve the anti-leukemic effects towards leukemia-stem like cells ($CD34^+CD38^-$ cell lines and $CD34^+$ primary samples). The rationale for exploring this drug combination with idarubicin and AT-101 is based on the fact that Bcl-2 is strongly associated with chemotherapy resistance [13,14] and thus inhibition of anti-apoptotic Bcl-2 family members with AT-101 might represent an attractive and promising avenue strategy to overcome the resistance of LSCs to conventional anticancer therapy.

In the present study, we report that AT-101 in combination with IDA has a synergetic and selective anti-AML activity *in vitro* against leukemia stem-like cell lines (i.e., $CD34^+CD38^-$ KG-1α and $CD34^+CD38^-$ Kasumi-1), as well as effective in $CD34^+$ primary AML patient samples *ex vivo* especially those with AML1/ETO, while sparing normal cells. In addition, we also obtain encouraging results from patient-derived xenograft murine models *in vivo*. Mechanistically, these events might attribute to the blockade of DNA repair and subsequent triggering of intrinsic apoptotic pathway. Thus, our study provides a theoretical basis to facilitate the development of a novel combinatorial approach to treat patients with AML.

2. Materials and methods

2.1. Chemicals and reagents

AT-101, idarubicin, Z-VAD-fmk are all purchased from MedChemExpress (Shanghai, China) and dissolved in DMSO.

2.2. Cell culture

The human AML cell line KG-1α is kindly provided from Dr. Pentao Liu of the University of Hong Kong, China and cultured with Iscove's Modified Dulbecco's medium (HyClone, Thermo Scientific, Waltham, MA, USA) supplemented with 10% fetal bovine serum (FBS, PAN Seratech, Aidan Bach, Germany) and 100 U/ml penicillin and 100 μg/ml streptomycin (1 × P/S, HyClone) at 37 °C in a humidified environment with 5% CO_2. Kasumi-1 cell line is provided by Union Hospital, Fujian Medical University (Fuzhou, China) and cultured in RPMI-1640 (HyClone, Thermo Scientific, Waltham, MA, USA) supplemented with 10% FBS and 1 × P/S. All cells were subjected to mycoplasma test every 2 months using MycoAlert mycoplasma detection kit (catalog no. LT07318; Lonza, USA).

2.3. Primary samples

Primary samples from bone marrow of AML patients (n = 18) and peripheral blood of healthy donors for hematopoietic stem cell transplantation (n = 8) are kindly provided by Department of Hematology, Nanfang Hospital, Southern Medical University and Department of Hematology, First Affiliated Hospital of Xiamen University. This study is carried out in accordance with the Declaration of Helsinki, and approved by the Ethics Review Board of Nanfang Hospital and First Affiliated Hospital of Xiamen University. Clinical characteristics of patients with AML are summarized in Table 1. Mononuclear cells were isolated by density gradient centrifugation using Lymphoprep TM (BD, Franklin Lakes, NJ, USA) and supplemented with 1 × P/S and 10% FBS for short culture.

2.4. Cell sorting

$CD34^+$ primary AML cells were isolated by the positive selection of CD34 using an immunomagnetic separation kit (MiniMACS CD34 Isolation kit; Miltenyi Biotec Gmbh, Bergisch Gladbach, Germany) according to the manufacturer's instructions. During the sorting procedure, cells were kept at 4 °C.

For cell line sorting, KG-1α and Kasumi-1 cell lines were stained with CD34-APC (clone 581, Biolegend, USA) and CD38-PE (clone HB-7, Biolegend, USA) for 30 min at 4 °C and washed twice with PBS supplemented with 2% FBS. Then the cells were sorted by flow cytometry (FACS Aria IIU, BD).

2.5. CCK-8 assay

Anti-proliferative effect was determined by a CCK-8 kit (MCE, Shanghai, China). Briefly, cells (3×10^4 cells/well) were plated into 96-well plates containing 100 μl of growth medium and then treated with designated doses of AT-101 or IDA or their combination for 24 h. CCK-8 agent was added and incubated for 2–4 h in an incubator after treatment and the absorbance at 450 nm were read by a VERSA max microplate reader (Molecular Devices, Sunnyvale, CA, USA). All experiments were repeated three times and performed in triplicate in each experiment. Combination indexes (CI) were calculated using CalcuSyn software (Biosoft, Cambridge, UK).

2.6. Apoptosis assays

Apoptosis assay was performed using an Annexin V Staining Kit (Thermofisher, USA) following the manufacturer's instruction. In brief, cells exposed to different treatments were harvested and washed with ice-cold PBS (Gibco, USA) and 1 × Annexin V binding buffer, and then analyzed by FACS Fortessa (BD Bioscience, Oxford, UK) and Flowjo software (TreeStar, San Carlos, CA) after Annexin V-FITC/PI staining. Primary samples with spontaneous apoptosis > 30% in the absence of treatment were excluded. For analysis of the potential relationship between patients' characteristics and *ex vivo* efficacy of AT-101/IDA, specific apoptosis was adopted to adjust the variation in basal levels of spontaneous cell death following the formula: (% apoptosis in treated cells − % apoptosis in untreated cells)/(1 − % apoptosis in untreated cells) [23].

2.7. Analysis of mitochondrial membrane potential

Mitochondrial membrane potential was evaluated using a JC-1 kit (Signalway Antibody, Pearland, TX, US) as described by the manufacturer. After exposed to the designed treatments cells were collected and incubated with 500 μl JC-1 staining working solution for 25 min in a 37 °C, 5% CO_2 incubator in the dark, and then subjected to flow cytometric analysis using Novocyte (ACEA Bioscience, San Diego, CA, USA) after washing.

2.8. Western blot analysis

Following various treatments, as described in figure legends, cells were harvested and lysed in RIPA buffer (Thermo Scientific, USA) supplemented with protease inhibitor (Roche Diagnostics, Mannheim, Germany) and phosphatase inhibitor (Roche Diagnostics, Mannheim, Germany). The protein level of each sample was quantified and normalized by a BCA protein Assay (Pierce, Thermo Scientific, USA). Equal amount of protein (20 μg/lane) was separated by SDS-PAGE, transferred to a PVDF membrane (Millipore, UK), blocked by 5% non-fat milk, and incubated with primary antibodies (all from Cell Signaling Technology, Danvers, MA, USA). After incubation with HRP-conjugated secondary antibodies, the signals were detected using an enhanced ECL substrate (GE Healthcare, Chicago, USA) and visualized using the

Table 1
Clinical characteristics of AML patients (n = 18).

Patient No.	Gender	Age	FAB	WBC ($\times 10^9$/L)	Blasts (%)	Cytogenetics	Molecular mutations	Induction therapy	Status after induction therapy
1	F	62		137.37	78.5	46, XX	U	IA	NR
2	F	29	unclassified	154.73	74	46, XX	U	IA	NR
3	M	32	M2	54.04	31	U	CBFβ-MYH11, FLT3-ITD	IA	CR
4	M	39	M2	14.13	53	46, XY	CEBPA	IA	CR
5	F	27	M2	4.33	24	46, XX, t(8; 21) (q22; q22)	AML1-ETO	IA	–
6	M	42		32.5	75	46, XY, t(11, 17) (q23; q12)	p53, MLL	IA	CR
7	M	68	MDS-AML	134.75	66	46, XY	U	DAC + CAG	–
8	M	22		3.93	31.5	46, XY, t(8; 21) (q22; q22)	CEBPA, AML1-ETO	IA	CR
9	M	16	M2	61.4	52	46, XY	FLT3-ITD	DA	CR
10	F	22	unclassified	111.84	27.5	46, XX	FLT3-ITD	IA	CR
11	F	47	M4	12.9	76	46, XX	U	IA	CR
12	M	44	M2	2.9	72	46, XY, t(8; 21) (q22; q22)	AML1-ETO	DA	CR
13	M	41	M2	29.52	68.5	46, XY	CEBPA	IA	CR
14	M	44	M2	5	25	45, X, -Y, t(8; 21) (q22; q22) [15] /46, XY [5]	AML1-ETO	IA	–
15	F	16	M1	18.2	34	46, XX, t(8; 21) (q22; q22)	AML1-ETO, NRAS	IA	CR
16	M	58	MDS-AML	94.81	62.5	46, XY	U	DAC + CAG	NR
17	M	36	M4	157.76	75	46, XY	U	DA	CR
18	M	26	M1	2.52	96	46, XY, del(11) (q23) [10] /46, XY [3]	CEBPA, MLL	IA	NR

Abbreviations: AML, acute myeloid leukemia; MDS, myelodysplastic syndrome; FAB, French-American-British subtype; IA, Idarubicin + Cytarabine; DA, Daunorubicin + Cytarabine; DAC, Decitabine; CAG, Cytarabine + Aclarubicin + G-CSF; CR, complete remission; NR, no remission. U, unknown.

Amersham Imager 600 (AI600, GE Healthcare, Chicago, USA).

2.9. Measurement of Ser 139-phosphorylated H2AX histone (γH2A.X)

For confocal microscopy, cells were collected and fixed with 4% paraformaldehyde for 15 min at room temperature. After permeabilization with 0.1% Triton X-100 (Sigma-Aldrich) and block with blocking buffer (Beyotime, Shanghai, China), cells were incubated with primary antibody (anti-γH2AX, 1:100, Cell Signaling Technology, Cat#9718S) at 4 °C overnight, and then stained with Alexa Fluor 555-conjugated donkey anti-rabbit secondary antibody (Invitrogen, USA) and phalloidin-FITC (Beyotime Biotechnology, China) for 2 h at room temperature in the dark. After that cells were dropped in glass slides and mounted using SlowFade Diamond Antifade Mountant with DAPI (Invitrogen, USA), and then scanned, photographed using a 100 × objective on Zeiss LSM780 confocal microscope (Zeiss, Jena, Germany).

For flow cytometry analysis, cells were harvested, fixed and permeabilized. After that cells were incubated with diluted Phospho-Histone H2A.X antibody (AF647 conjugate) (1:200, Cell Signaling Technology, Cat#9720S) for 1 h at room temperature, and then subjected to Novoctye.

2.10. Alkaline comet assay

Following treatment with AT-101, IDA, both, or neither for 6 h, AML cells were subjected to alkaline comet assays using a Comet Assay Kit (Abcam, Cambridge, UK) according to the manufacturer's instruction. First, the comet slides were coated with normal-melting-point agarose to form a base layer. After that, a mixture of cells and comet agarose was applied as the second layer. Comet slides were immersed in cold fresh lysis solution for 2 h at 4 °C, and then transferred to a container pre-filled pre-chilled Alkaline Solution for 30 min at 4 °C in order to loosen the tight double-helical structure of DNA. The slides were then rinsed twice by distilled water and stained with Propidium Iodide after electrophoresis was performed at 300 mA for 25 min in Alkaline electrophoresis solution. Last, comets were viewed using a Nikon TI-U fluorescence microscope and analyzed by CASP software (CASP, Wroclaw, Poland). The Percentage of DNA in the comet tail was recorded from at least 100 comets to characterize the DNA damage.

2.11. Measurement of intracellular ROS

ROS was detected using a Total Reactive Oxygen Species (ROS) Assay Kit (Thermofisher, USA) following the manufacturer's instruction. In brief, cells were harvested after AT-101 (2 μM) or IDA (20 nM) or their combination for indicated hours and then incubated with 100 μl ROS assay buffer supplemented with 0.2 μl ROS assay stain for 60 min in a 37 °C, 5% CO_2 incubator in the dark, and then subjected to flow cytometric analysis.

2.12. Animal studies in patient-derived xenograft models

The animal studies were approved by Xiamen University Animal Care and Use Committees. 16 male NOD-Prkdc$^{-/-}$IL2rg$^{-/-}$ mice (NPI, IDMO ltd., Beijing, China) were intravenously injected with 2×10^6 splenic cells of humanized xenograft mice generated from an AML patient carrying FLT3-ITD mutation via tail vein after irradiation (1 Gy). After confirmation of engraftment by human CD45 staining in peripheral blood, mice were randomly assigned to four groups (n = 4/group) and given either vehicle control or idarubicin alone (0.5 mg/kg, i.v., day 1–3 only), AT-101 alone (50 mg/kg, oral gavage, day 1–10), or their combination. At the end of the experiments, mice were euthanized and the leukemia burden in spleen and peripheral blood was determined by flow cytometry after staining with human CD45-FITC (clone HI30, Biolegend) and murine CD45-BV421 antibodies (clone 30-F11, Biolegend). Livers and lungs from mice receiving treatments were fixed in 4% paraformaldehyde for 24 h, after which paraffin-embedded sections were prepared and subjected to H&E staining and immunohistochemistry (IHC).

2.13. Immunohistochemical staining

Paraffin-embedded livers and lungs were sectioned and deparaffinized with 100% xylene, and then subjected to rehydration with different concentrations of alcohol. Tissue slides were immersed in boiling citrate buffer for 30 min for antigen retrieval and incubated with primary antibody against human CD45 (Cell Signaling Technology, Cat#13917S) overnight at 4 °C after blocking with 3% BSA solution. After washing, HRP polymer conjugate reagent and DAB

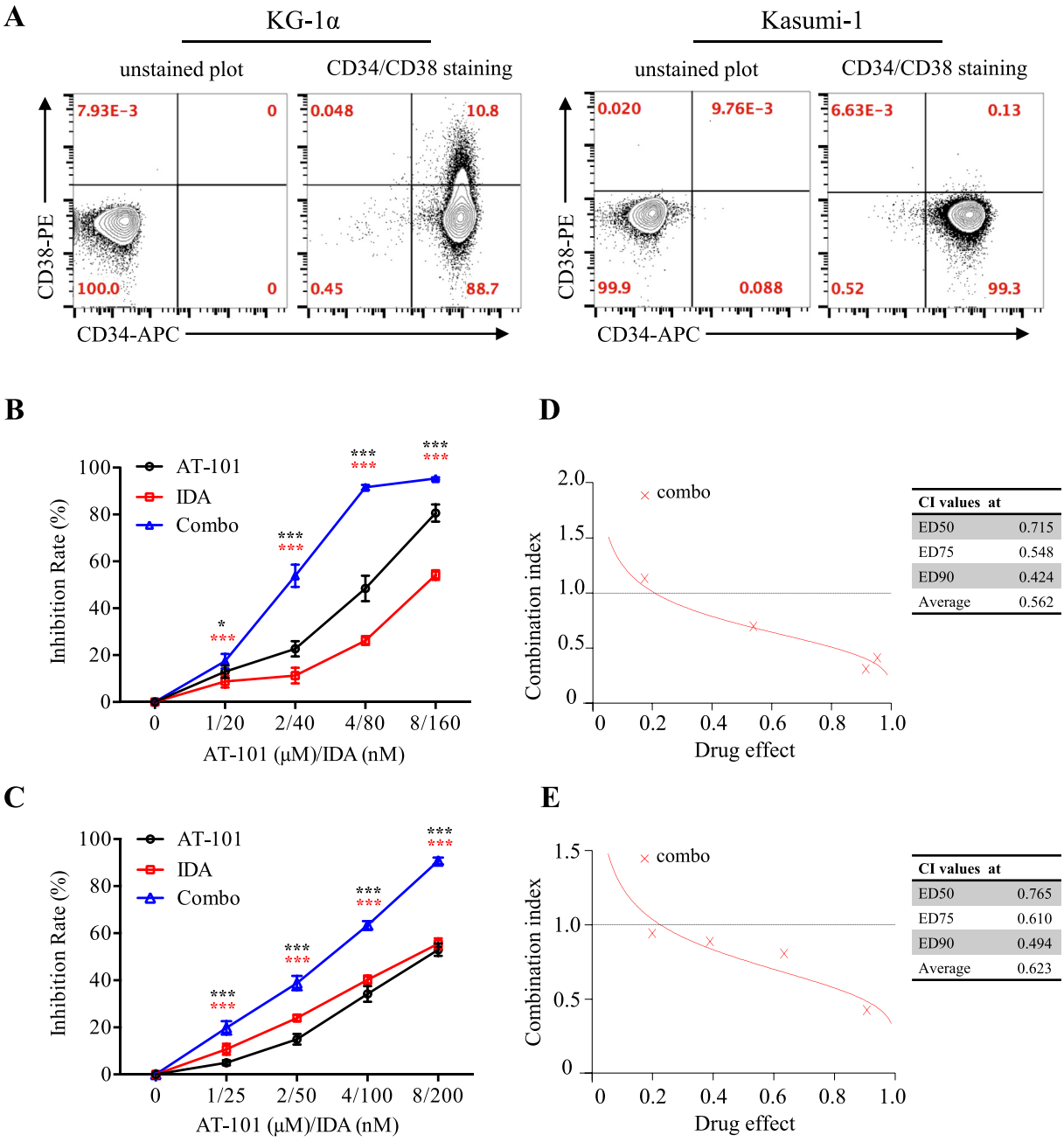

Fig. 1. Combination of AT-101 and IDA results in synergistic inhibition of proliferation in LSC-like cells *in vitro*. (A). $CD34^+/CD38^-$ percentage in KG-1α (left panel) and Kasumi-1 (right panel) was shown. **(B–C).** $CD34^+CD38^-$ KG-1α cells (B) and $CD34^+CD38^-$ Kasumi-1 cells (C) were treated with the indicated concentrations of AT-101 and IDA for 24 h, and then subjected to CCK-8 assay for detection of the anti-proliferative effect. **(D-E).** CI plots of AT-101/IDA combinatorial treatment in LSC-like cell lines $CD34^+CD38^-$ KG-1α (D) and $CD34^+CD38^-$ Kasumi-1 (E). Black asterisk indicated the statistical significance between combo (refer to the combination of AT-101 and IDA) and AT-101; red asterisk indicated the statistical significance between combo and IDA. *p < 0.05, **p < 0.01, ***p < 0.001. (For interpretation of the references to colour in this figure legend, the reader is referred to the Web version of this article.)

chromogen were added and hematoxylin solution was used for counterstaining. Finally, slides were dehydrated, air-dried, mounted and photographed. For hematoxylin and eosin staining (H&E staining), slides were immersed in a coplin jar containing Mayer's hematoxylin solution, washed with distilled water and counterstained with eosin Y solution. Images were taken using an optical microscope under the same magnification.

2.14. Statistical analysis

Statistical analysis was assessed by one-way or two-way analysis of variance (ANOVA) followed by LSD posthoc test with Prism software v6.0 (GraphPad Software, La Jolla, CA, USA). The accepted level of statistical significance was $P < 0.05$.

3. Results

3.1. Combination of AT-101 and IDA results in synergistic inhibition of proliferation in LSC-like cells in vitro

First, the $CD34^+CD38^-$ cell population in two leukemia stem-like cell lines (LSC-like cells) KG-1α and Kasumi-1 was shown in Fig. 1A. To

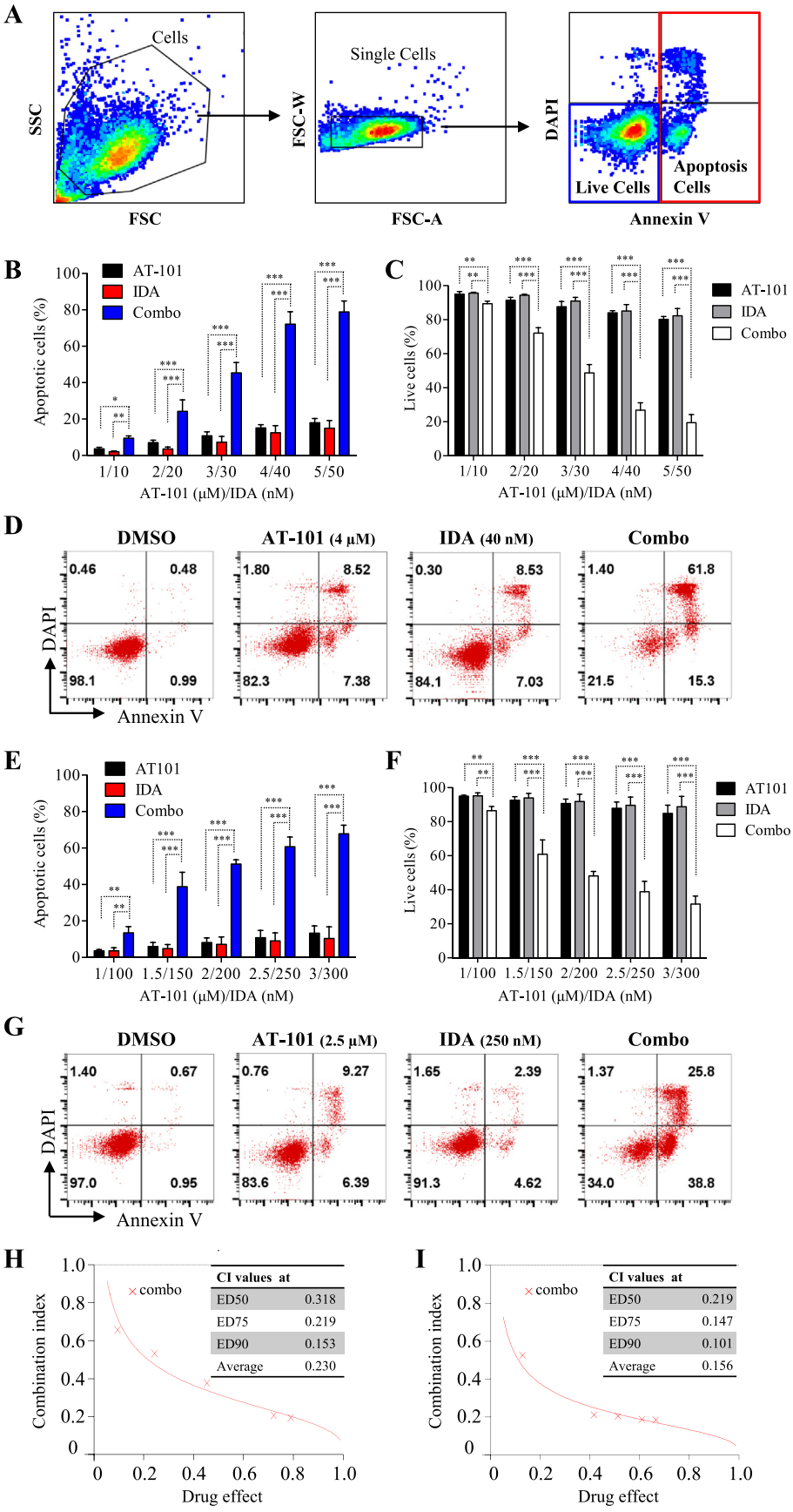

Fig. 2. Combination of AT-101 and IDA results in synergistic induction of apoptosis in LSC-like cells *in vitro*. **(A).** Flow cytometric plots showing the gating strategy to determine the percentages of apoptotic cells (Annexin V^+) and live cells (Annexin V^-/DAPI$^-$). **(B–C).** $CD34^+CD38^-$ KG-1α cells were exposed to the indicated concentrations of AT-101 and IDA for 24 h, after which percentages of apoptotic cells (B) and live cells (C) were determined. **(D).** Representative flow cytometric data for Annexin V/DAPI staining in $CD34^+CD38^-$ KG-1α cells. **(E-F).** $CD34^+CD38^-$ Kasumi-1 cells were exposed to the indicated concentrations of AT-101 and IDA for 24 h, after which percentages of apoptotic cells (E) and live cells (F) were determined. **(G).** Representative flow cytometric data for Annexin V/DAPI staining in $CD34^+CD38^-$ Kasumi-1 cells. **(H–I).** CI plots of AT-101 combined with IDA concomitant treatment in LSC-like cell lines $CD34^+CD38^-$ KG-1α (H) and $CD34^+CD38^-$ Kasumi-1 (I). *p < 0.05, **p < 0.01, ***p < 0.001.

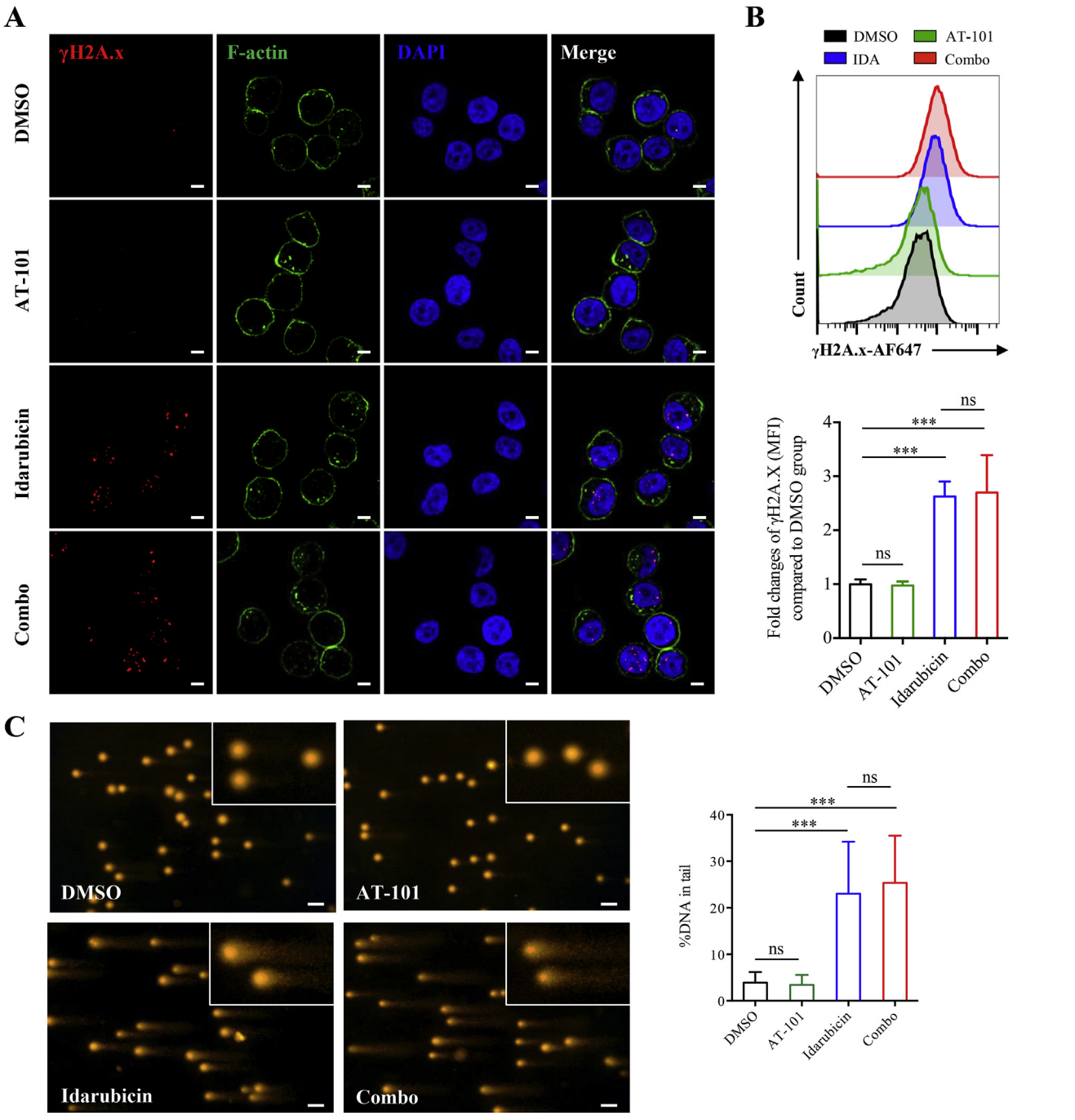

(caption on next page)

Fig. 3. AT-101 blocks DNA damage repair upon DNA-damaging drug treatment. $CD34^+CD38^-$ KG-1α cells were treated with AT-101 (2 μM) or IDA (20 nM) or their combination for 6 h. **(A).** Confocal immunofluorescence assay was performed after stained with anti-phospho-Histone H2A.X (Ser139) antibody (red), phalloidin probe (green) and DAPI (blue). Scale bars, 5 μm. **(B).** Flow cytometric analysis for detection of γH2AX was carried out after stained with a fluorescence-conjugated antibody. (C). Comet assay was performed to further conclude DNA damage. **(D).** Levels of *p*-ATM, ATM, *p*-ATR, ATR, *p*-Chk2, Chk2, *p*-Chk1, Chk1 and Rad51 were assessed using western blotting after $CD34^+CD38^-$ KG-1α cells were treated with AT-101 (2 μM) or IDA (20 nM) for 24 h. GAPDH was used as a loading control. $^*p < 0.05$, $^{**}p < 0.01$, $^{***}p < 0.001$. (For interpretation of the references to colour in this figure legend, the reader is referred to the Web version of this article.)

evaluate the combinatorial effect of AT-101 and IDA on cell proliferation in LSC-like cells, we treated $CD34^+CD38^-$ KG-1α and $CD34^+CD38^-$ Kasumi-1 cells with indicated concentrations of AT-101 and IDA for 24 h and measured cell proliferation by CCK-8 assay. The results showed that exposure to both AT-101 (black lines) and IDA (red lines) single treatment significantly inhibited KG-1α proliferation in a dose-dependent manner, however, co-administration of AT-101 and IDA (blue lines) resulted in a further increased inhibition of cell proliferation (Fig. 1B). Similar results were obtained with Kasumi-1 cells (Fig. 1C). Combination index (CI) was used for the synergy quantification of drug combinations, as it offered a quantitative definition for additive effect (CI = 1), synergism (CI < 1), and antagonism (CI > 1) based on the ChouTalalay method [24]. CI values were calculated by Calcusyn software and the synergism effects were observed in these two LSC-like cell lines as shown in Fig. 1D and E, evidenced by all CI values at $ED_{50}/ED_{75}/ED_{90} < 1$. In addition, dynamic cell growth curves upon drug treatment were also evaluated by absolute cell counting. As shown in Fig. S1, co-treatment with AT-101/IDA further eradicated the leukemia burden in both two LSC-like cell lines compared to two single agent groups.

3.2. Combination of AT-101 and IDA results in synergistic induction of apoptosis in LSC-like cells in vitro

Next, in order to further confirm the cytotoxicity effect of AT-101 and IDA when used in combination, we treated $CD34^+CD38^-$ KG-1α cells with AT-101 at various concentrations (1–5 μM) in the presence or absence of different concentrations of IDA (10–50 nM) for 24 h and then measured cell death by Annexin V/DAPI dual staining. The percentage of dead cells (i.e., Annexin V^+) and live cells (i.e., Annexin $V^-/DAPI^-$) were determined by FACS analysis, and representative plots for gating strategy was shown in Fig. 2A. The results showed that, even though exposure to a series of dosages of AT-101 and IDA single treatment can induce some extent of apoptosis (~20%) and a reduction of live cells in KG-1α cells, these events were drastically enhanced by combined treatment for 24 h (all $P < 0.05$ for each combinatorial doses, Fig. 2B and C), of which representative flow cytometric data was shown in Fig. 2D. Comparable phenomena were also observed in $CD34^+CD38^-$ Kasumi-1 cells (Fig. 2E–G). In addition, strong synergism effects were also observed in these two LSC-like cell lines as indicated by all CI values < 1 (Fig. 2H and I), which in line with our CCK-8 results.

3.3. AT-101 blocks DNA damage repair upon DNA-damaging drug treatment

DNA damage response (DDR) is one of the most attractive targets in cancer therapies [25,26]. Modulation of DDR network can alter the response of cancer cells to DNA damaging anti-cancer drugs, such as idarubicin, which is one of the most important cell death mechanisms induced by chemotherapy agents [27,28]. H2AX, a member of the histone H2A family, is rapidly phosphorylated at serine 139 at the sites of DNA damage. This very early event in the response of mammalian cells to DNA double-strand breaks precedes the actions of DNA repair enzymes, and thus serves as a sensitive marker for detection of DNA damage. Therefore, we measured Ser139 phosphorylation of H2AX (designated γH2AX) by confocal immunofluorescence microscopy and FACS analysis. As shown in Fig. 3A and Fig. S2, confocal microscopy analysis showed that 6 h' AT-101 treatment alone did not induce a detectable γH2AX in $CD34^+CD38^-$ KG-1α cells, whereas administration with IDA alone or AT-101/IDA combined treatment for 6 h resulted in an abrupt increase in levels of γH2AX, consistent with the fact of that IDA was an effective DNA damaging drug. The above results were further supported by the quantitative flow cytometric assessment of γH2AX (Fig. 3B) and comet assay (Fig. 3C), where IDA alone and combination treatment induced a much higher γH2AX level. Generally, the DNA repair response is activated in response to DNA damage. Hence, we also assessed the important proteins involved in the DNA repair response in $CD34^+CD38^-$ KG-1α cells by western blot. As shown in Fig. 3D, AT-101 alone or the AT-101/IDA combinatorial therapy significantly reduced the activity of DNA damage response, reflected by a marked decrease in total/phosphorylation levels of DNA damage repair proteins ATM, ATR, Rad51, as well as the DNA damage response proteins Chk1 and Chk2. Of note, in the combination group, addition of AT-101 even diminished the IDA-induced elevation of Rad51, Chk1, and Chk2.

Considering that DNA damage was closely associated with the formation of free radical and oxidative stress, therefore, quantification of total ROS in drug-treated $CD34^+CD38^-$ KG-1α cells was also performed. As shown in Fig. S3, exposure to AT-101 at 6 or 12 or 24 h had almost no effect on the generation of ROS. In contrast, either treatment with IDA or combination treatment did not trigger the intracellular ROS at 6 or 12 h while significantly induced ROS at 24 h, which lagged behind the accumulation of DNA damage (early to 6 h).

Therefore, our data suggested that AT-101 repressed the DNA repair activity thus preventing leukemia cells from repairing chemotherapy-induced DNA damage, which might account for the synergistic effects of AT-101 with IDA to induce cell death of LSC-like cells.

3.4. Synthetic lethality of AT-101/IDA depends on the activation of intrinsic apoptotic pathway

Reduced mitochondrial membrane potential is considered as an initial and irreversible progression towards apoptosis. To further investigate the mechanism of cell death triggered by AT-101/IDA, mitochondrial membrane potential (ΔΨm) was analyzed by flow cytometry using the JC-1 probe in $CD34^+CD38^-$ KG-1α cells after treatment with AT-101 (4 μM) or IDA (100 nM) or their combination. The results showed that co-administration of AT-101 and IDA for 12 h robustly induced more mitochondrial membrane depolarization compared to other treatments (Fig. 4A and B). It is well accepted that caspase activation plays a central role in the execution of apoptosis. Thus, we wonder whether addition of Z-VAD-fmk (pan-caspase inhibitor) to block the activation of caspase could rescue the apoptosis induced by the combinatorial treatments. To this end, apoptotic status was analyzed after 24 h' exposure to AT101 or IDA or the combination in the presence or absence of Z-VAD-fmk (20 μM). As shown in Fig. 4C, treatment with Z-VAD-fmk alone did not trigger apoptosis (green columns), and was unable to rescue apoptosis induced by IDA (red columns). In contrast, Z-VAD-fmk slightly salvaged the AT-101-induced apoptosis (black columns), while tremendously rescued apoptosis induced by AT-101/IDA combined treatment (blue columns) in $CD34^+CD38^-$ KG-1α cells, of which representative flow cytometric data was shown in Fig. 4D. Similar results were obtained in another LSC-like cell line, $CD34^+CD38^-$ Kasumi-1 (Fig. 4E and F). In addition, western blot analysis (Fig. 4G and H) revealed that treatment with IDA alone had no effect on the expression of anti-apoptotic proteins,

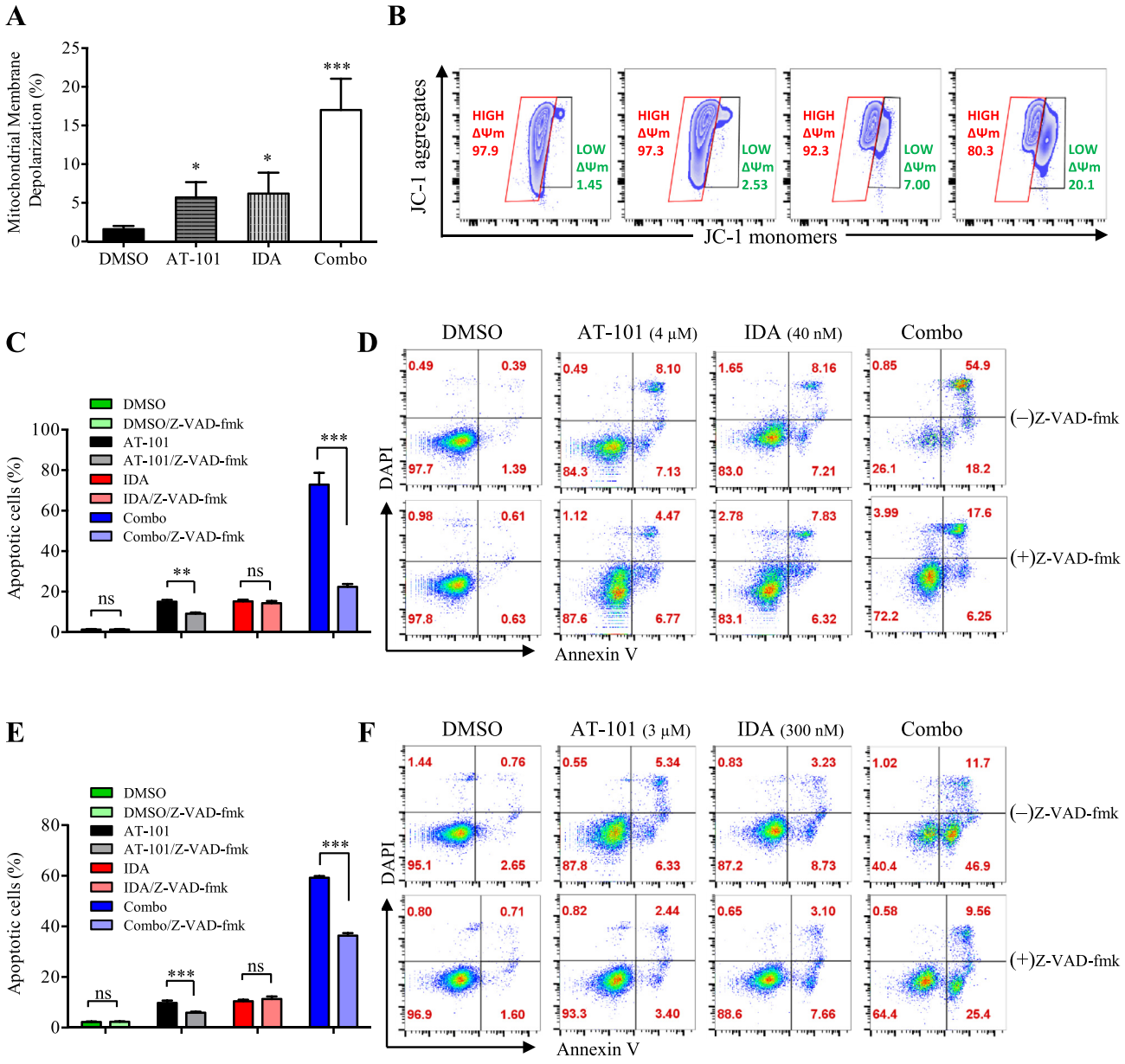

(caption on next page)

Fig. 4. Synthetic lethality of AT-101/IDA depends on the activation of intrinsic apoptotic pathway. **(A-B).** $CD34^+CD38^-$ KG-1α cells were exposed to AT-101 (4 μM) or IDA (100 nM) or their combination for 12 h, after which mitochondrial membrane potential (ΔΨm) was measured by flow cytometry using a JC-1 kit. **(C–F).** Apoptotic status of $CD34^+CD38^-$ KG-1α (C–D) and $CD34^+CD38^-$ Kasumi-1 (E–F) were measured by Annexin V/DAPI staining after pretreatment with 20 μmol/L Z-VAD-fmk for 2 h, followed by the indicated concentrations of AT-101 and IDA for additional 24 h. **(G).** Protein levels of Bcl-2, Mcl-1, Bcl-xL, XIAP and PARP/cleaved PARP were assessed using western blotting after treatment with AT-101 (2 μM) or IDA (20 nM) for 24 h in $CD34^+CD38^-$ KG-1α cells. GAPDH was used as a loading control. (H). Immunoblot analysis for caspase 3 and cleaved caspase 3 in $CD34^+CD38^-$ KG-1α cells. β-actin was used as a loading control. *$p < 0.05$, **$p < 0.01$, ***$p < 0.001$.

including Bcl-2, Mcl-1, Bcl-xL and XIAP, while either exposure to AT-101 or the combination led to a marked degradation, accompanied by the cleavage of PARP and caspase 3, which were hallmarks of mitochondrial apoptosis. Taken together, these findings indicate that AT-101/IDA-induced apoptosis in LSC-like cells is highly dependent on the activation of intrinsic apoptotic pathway, at least in part, due to the down-regulation of anti-apoptotic proteins.

3.5. AT-101/IDA preferentially targets AML1/ETO-positive primary $CD34^+$ AML cells while sparing normal hematopoietic cells ex vivo

Next, in order to further evaluate the activity of AT-101/IDA on LSC-like cells, $CD34^+$ primary cells were isolated from AML patients and healthy donors by magnetic activated cell sorter (MACS), respectively. Clinical characteristics of AML patients are summarized in Table 1. Purified $CD34^+$ AML cells and $CD34^+$ normal hematopoietic cells were treated with AT-101 (5 μM) in the presence or absence of 20 nM IDA for 24 h, and then subjected to Annexin V/PI dual staining. The percentage of apoptotic cells was determined using FACS analysis. In agreement with the *in vitro* anti-leukemia effects observed in LSC-like cell lines, exposure to the combined treatment resulted in a robust increase in apoptosis in $CD34^+$ AML cells compared to single treatment (Fig. 5A; $P < 0.0001$ and $P = 0.0012$, Combo versus AT-101 and IDA, respectively; $n = 18$), even though treatment with AT-101 alone and IDA alone both induced apoptosis ($P = 0.0078$ and $P = 0.0004$, AT-101 and IDA versus DMSO control, respectively). Representative flow cytometric data of primary AML (patient No.12) after drug exposure was also shown in Fig. 5B. Of note, AT-101 and IDA combined treatment displayed minimal toxicity towards $CD34^+$ normal hematopoietic cells under the same conditions (Fig. 5C; all $P > 0.05$ for AT-101/IDA/Combo versus DMSO control). Together, these findings suggested that AT-101/IDA selectively induced apoptosis of primary $CD34^+$ AML cells while largely spared normal hematopoietic stem cells.

Considering the heterogeneity in response to the combined treatment, we wondered whether the clinical features of AML patients would affect the anti-leukemia activity of AT-101/IDA against primary AML cells. To this end, we analyzed the potential relationship between patients' characteristics and the percentage of apoptosis induced by AT-101/IDA. Specific apoptosis was adopted here in order to normalize the marked difference in basal levels of spontaneous cell death of primary samples. As shown in Table S1, two-way ANOVA analysis revealed that the *ex vivo* efficacy of AT-101/IDA in primary AML cells was significantly associated with the status of AML1/ETO in AML patients ($P = 0.0005$, AML1/ETO-positive vs AML1/ETO-negative). However, other clinical features (e.g., hyperleukocytosis, FLT3-ITD, CEBPA) did not significantly affect the response of primary AML cells to AT-101/IDA combined treatment (all $P > 0.05$).

3.6. AT-101/IDA suppresses tumor growth in vivo in patient-derived xenograft models of FLT3-ITD mutant AML

Last, we tested the efficacy of AT-101/IDA *in vivo* using an established patient-derived xenograft models. PDX cells were obtained from mouse spleens of primary humanized xenografts which generated from a primary $FLT3\text{-}ITD^{mut}$ AML patient, and then transplanted into irradiated NOD-$Prkdc^{-/-}IL2rg^{-/-}$ mice (See Materials and Methods section for more details about engraftment). Schematic outline of the *in vivo* experiment was depicted in Fig. 6A. Mice were randomly assigned into four groups ($n = 4$/group) and treated with vehicle, AT-101 (50 mg/kg, 10 days, p.o.), IDA (0.5 mg/kg, 3 days, i.v.) or the combination after confirmation of engraftment by hCD45 staining in peripheral blood (Fig. 6B; all $P > 0.05$ among treatment groups). As shown in Fig. 6C and 50 mg/kg AT-101 monotherapy did not decrease the weight of spleens ($P = 0.3915$, AT-101 versus Vehicle), and IDA (0.5 mg/kg) alone moderately improved the disease-associated splenomegaly ($P = 0.0079$, IDA versus Vehicle). However, splenomegaly was dramatically reduced by the combination treatment ($P = 0.0001$, Combo versus Vehicle; $P = 0.0094$, Combo versus IDA). Meanwhile, leukemia burden was also assessed in spleen and peripheral blood by FACS. Combined treatment markedly attenuated AML growth, reflected by diminished human $CD45^+$ cells in spleens (Fig. 6D; $P < 0.0001$, Combo versus Vehicle; $P = 0.001$, Combo versus IDA) and peripheral blood (Fig. 6E; $P < 0.0001$, Combo versus Vehicle). Representative data for detection of human $CD45^+$ cells in spleens of PDX mice was shown in Fig. 6F. In addition, remarkable reduction of infiltrated leukemic cells was also observed in the livers (Fig. 6G) and lungs (Fig. 6H) of mice receiving the AT-101/IDA combinatorial therapy, as revealed by immunohistochemical (IHC) and HE staining.

4. Discussion

In recent years, increasing evidence has demonstrated that there is a rare population of LSCs in patients with AML, which are responsible for treatment failure due to their self-renewal and unlimited repopulating potential [5,6]. Cancer stem cells usually possess stronger capacity of DNA repair than bulk leukemia cells to maintain genomic integrity in response to the DNA-damaging chemotherapies [29,30]. Consequently, LSCs are hard to be eliminated with conventional chemotherapeutic drugs (daunorubicin, idarubicin), leading to dismal clinical outcomes for AML. Theoretically, there are two ways to overcome this difficulty. One is to employ higher doses of chemotherapeutic agents, however, severe or even lethal toxic side effects are the main concerns. The other approach is to combine chemotherapeutic agents with other effective compounds to boost their effects. In this preclinical study, we adopted two cell lines, $CD34^+CD38^-$ KG-1α and $CD34^+CD38^-$ Kasumi-1 cells, and $CD34^+$ primary cells from AML patients to evaluate the effect of combined therapy on LSC-like cells. We reported here that AT-101 and idarubicin (IDA) acted in synergy and induced vigorous cell death against LSC-like cells *in vitro* when used in combination. Moreover, this combined treatment was also highly effective *in vivo* in a human AML mouse PDX model.

DNA is the main target of cancer therapeutics whereby induction of DNA damage initiates a cascade of events that ultimately determines the fate of cancer cells [31,32]. Cell death following DNA damage depends on the amount of critical DNA damage and the DNA repair capacity of cells [33]. Under normal conditions, cells to respond to critical DNA damage is mainly detected by ATM and ATR, and then activate a series of downstream key nodes, for example, Chk2, Chk1 and Rad51, to prevent cell cycle progression and recruit DNA repair proteins to facilitate DSB repair [34–36]. The results of the present study elucidated that AT-101 diminished the DNA damage repair capacity of LSC-like cells, and thus prevented them from repairing IDA-induced violent DNA damage. Simultaneously, IDA-induced high level of DNA damage exceeded the DNA repair capacity which impaired by AT-101, leading

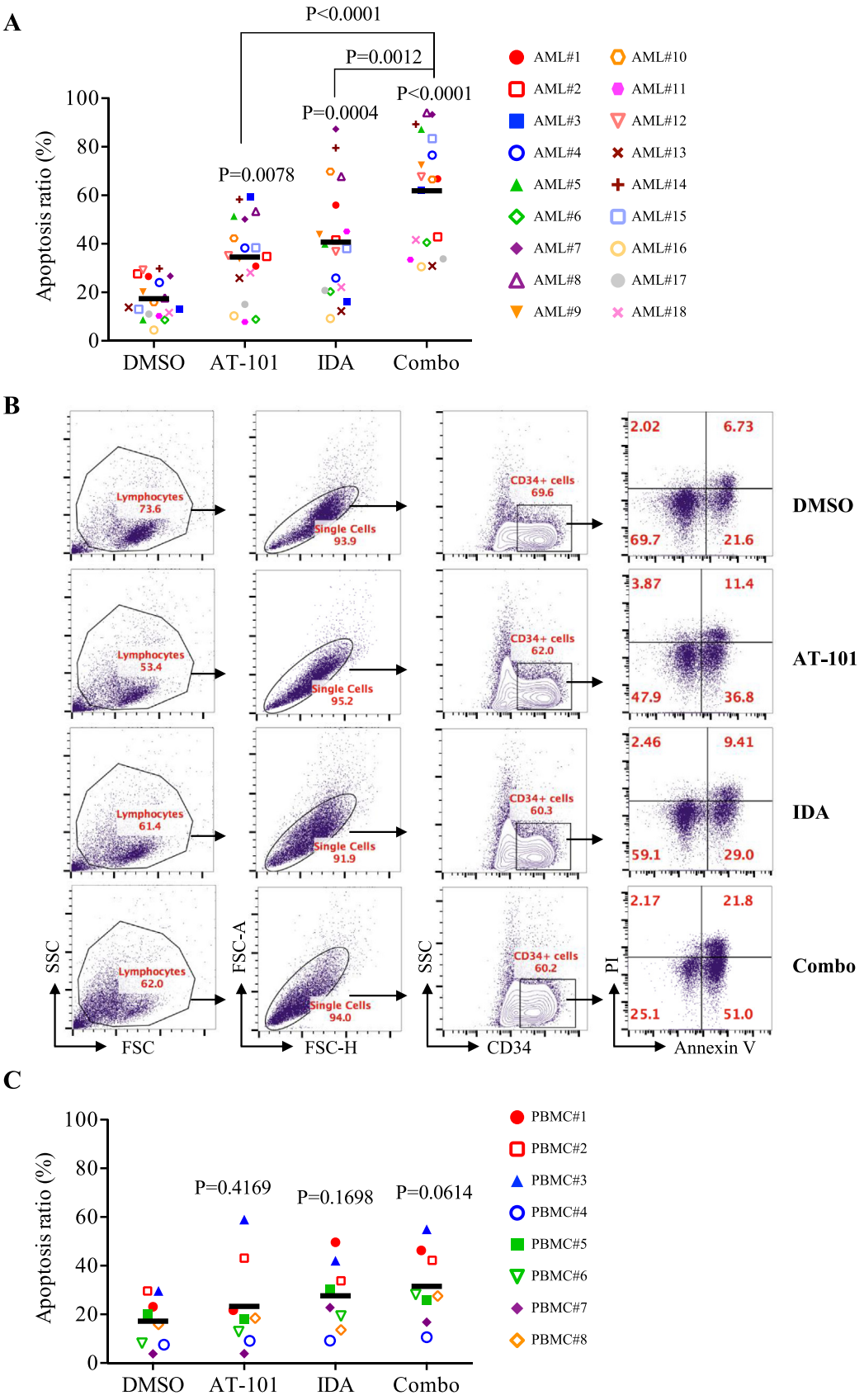

Fig. 5. AT-101/IDA preferentially targets AML1/ETO-positive primary CD34$^+$ AML cells while sparing normal hematopoietic cells *ex vivo*. **(A&C).** CD34$^+$ mononuclear cells of patients with AML (A) and healthy donors (C) were exposed to AT-101 (5 μM) or IDA (20 nM) or their combination for 24 h, and then flow cytometric analysis was carried out to detect the apoptotic cells (Annexin V$^+$). Each symbol represents result for an individual. Horizontal bold black lines represent the mean of apoptosis rates. **(B).** Representative flow cytometric data for CD34/Annexin V/DAPI staining in patient#12 after AT-101/IDA treatment.

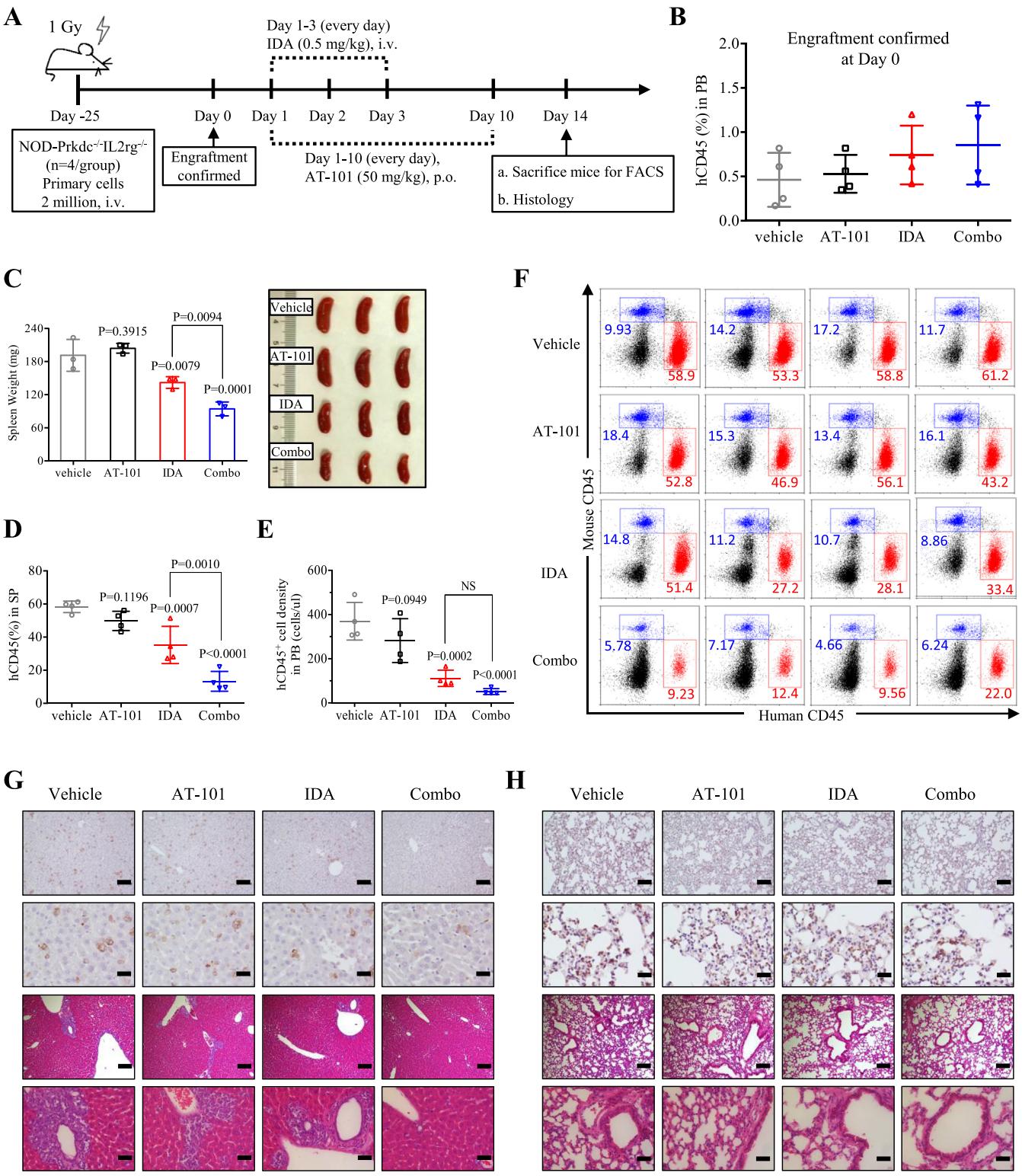

Fig. 6. AT-101/IDA suppresses tumor growth *in vivo* in patient-derived xenograft models of AML. **(A).** Schematic outline of the *in vivo* experiment of PDX models. **(B).** Confirmation of AML engraftment on day 0 (25 days after injection) by human CD45 staining. **(C).** Weight and image of representative spleens from sacrificed mice. **(D-E).** Leukemia burden in spleen (D) and peripheral blood (E) after treatments. **(F).** Representative data for flow cytometric analysis of mCD45/hCD45 staining in spleens. **(G-H).** Immunohistochemical staining for hCD45 and H&E staining of histologic sections of liver (G) and lung (H) in experimental mice. 1st Row: IHC 100 × , scale bar: 100 μm; 2nd Row: IHC 400 × , scale bar: 25 μm; 3rd Row: HE 100 × , scale bar: 100 μm; 4th Row: HE 400 × , scale bar: 25 μm.

to the activation of mitochondria-mediated intrinsic apoptotic pathway (Fig. 7). These events included the downregulation of anti-apoptotic proteins (Bcl-2, Mcl-1, Bcl-xL and XIAP), mitochondrial outer membrane permeabilization (loss of mitochondrial membrane potential), and following PARP degradation, ultimately inducing apoptosis of LSC-like cells.

It is well known that therapeutic response and prognosis of patients with AML are significantly affected by multiple risk factors. Among

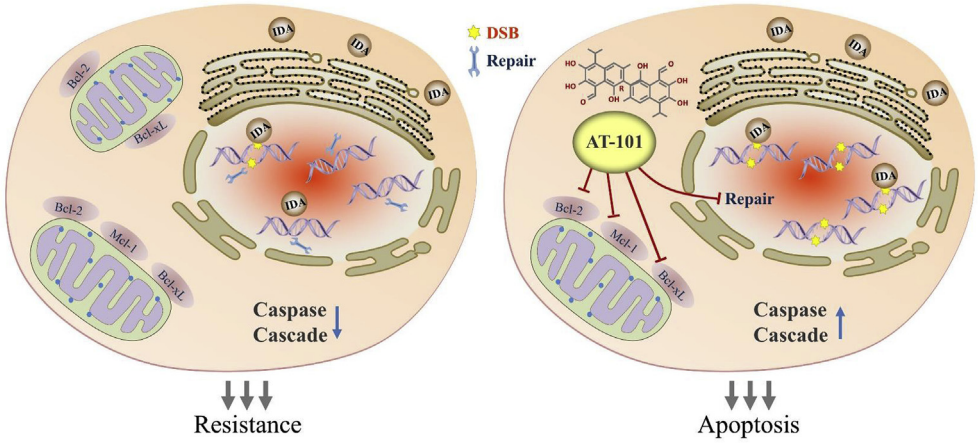

Fig. 7. The cytotoxicity of AT-101/IDA combinatorial treatment attribute to the blockage of DNA repair response and subsequent activation of intrinsic apoptotic pathway.

those, rearrangement between the AML1 and ETO genes (AML1/ETO) identifies a subgroup of AML patients with a relatively good prognosis which benefit from the conventional chemotherapy [37,38]. Interestingly, although the sample size and the molecular diversity of patients enrolled in this study was limited, our results indicated that the *ex vivo* cytotoxicity of AT-101/IDA combinatorial treatment was significantly associated with the patients' status of AML1/ETO (64.62% vs 36.75%, apoptosis rate of combined treatment in patients with AML1/ETO versus those without AML1/ETO), implying that patients carrying AML1/ETO might benefit from the combinatorial therapy. On the other hand, although hyperleukocytosis (peripheral white blood cell count exceeding 100,000/mm^3) [39,40] and status of FLT3-ITD mutation [41] were high-risk factors in AML, which were associated with greater incidence of disease-related deaths, the marked *ex vivo* activity of AT-101/IDA was still observed in patients with these two unfavorable factors, without statistical significance observed when compared with their respective counterparts (P = 0.9562, patients with hyperleukocytosis versus the counterpart; P = 0.2143, patients with FLT3-ITD versus the counterpart). This was partially verified by our *in vivo* results. In this pre-clinical study, bone marrow cells from a FLT3-ITD^{mut} patient were collected at disease relapse status after two cycles of MD-Arac, and then the PDX model was generated based on this AML patient. According to the NCCN AML Guidelines, patients carrying FLT3-ITD mutation should be considered for clinical trials where available due to the significant poorer outcomes upon conventional chemotherapy. Bracingly, AT-101 in combination with IDA significantly reduced leukemia burden in this FLT3-ITD^{mut} PDX model without hair or weight loss, which in agreement with the phenomena that patients with unfavorable factor FLT3-ITD might also be susceptible to this combinatorial therapy. However, these results might be controversial and remain to be explored in our successor studies.

In conclusion, our study demonstrated the synergistic activity of AT-101 and IDA combined treatment on LSC-like cell lines, primary AML cells, and human AML PDX models. Though the exact mechanisms of how AT-101/IDA treatment eradicate LSC-like cells remained to be defined, the results presented here suggested that combined therapy of AT-101/IDA might primarily act to block DNA repair by AT-101 and thus prevent LSC-like cells recovering from idarubicin-induced DNA damage and cell death. Therefore, this combination strategy warrants further clinical investigation in treatment of refractory and relapsed leukemia.

Ethics approval and consent to participate

Bone marrow aspirates of AML patients and peripheral blood of healthy donors were obtained with the informed consent for research purposes. This study was carried out in accordance with the Declaration of Helsinki, and approved by the Ethics Review Board of Nanfang Hospital and First Affiliated Hospital of Xiamen University.

Conflicts of interest

The authors declare no conflict of interest.

Author contributions

Conception and design: **QY, KC, LZ, BX.** Acquisition, analysis and interpretation of data: **QY, KC, LZ, GF, BX**. Development of methodology: **QY, KC, LZ, LY, GF, SJ, CL**. Primary samples collection and purification and validation: **SB, YZ, HZ**. Animal model analysis and data collection: **LF, GF, SJ, CL**. Writing, and revision of the manuscript: **QY, KC, XLC, GF, BX.**

Acknowledgements

This work was financially supported by National Natural Science Foundation of China, PR China (No.81570156, No.81770126, No.81770161).

Appendix A. Supplementary data

Supplementary data to this article can be found online at https://doi.org/10.1016/j.canlet.2019.07.003.

References

[1] H. Dohner, D.J. Weisdorf, C.D. Bloomfield, Acute myeloid leukemia, N. Engl. J. Med. 373 (2015) 1136–1152.
[2] E. Papaemmanuil, M. Gerstung, L. Bullinger, V.I. Gaidzik, P. Paschka, N.D. Roberts, N.E. Potter, M. Heuser, F. Thol, N. Bolli, Genomic classification and prognosis in acute myeloid leukemia, N. Engl. J. Med. 374 (2016) 2209–2221.
[3] W. Yingzi, A.V. Krivtsov, A.U. Sinha, T.E. North, G. Wolfram, F. Zhaohui, L.I. Zon, S.A. Armstrong, The Wnt/beta-catenin pathway is required for the development of leukemia stem cells in AML, Science 327 (2010) 1650–1653.
[4] L. Crews, L. Balaian, N. Delossantos, H. Leu, A. Court, E. Lazzari, A. Sadarangani, M. Zipeto, J. Laclair, R. Villa, RNA splicing modulation selectively impairs leukemia stem cell maintenance in secondary human AML, Cell Stem Cell 19 (2016) 599–612.
[5] L. Jin, K.J. Hope, Q. Zhai, F. Smadja-Joffe, J.E. Dick, Targeting of CD44 eradicates human acute myeloid leukemic stem cells, Nat. Med. 12 (2006) 1167–1174.
[6] R. Majeti, M.P. Chao, A.A. Alizadeh, W.W. Pang, S. Jaiswal, K.D.G. Jr, N.V. Rooijen, I.L. Weissman, CD47 is an adverse prognostic factor and therapeutic antibody target on human acute myeloid leukemia stem cells, Cell 138 (2009) 286–299.
[7] T. Lapidot, T. Grunberger, J. Vormoor, Z. Estrov, O. Kollet, N. Bunin, R. Zaizov, D.E. Williams, M.H. Freedman, Identification of human juvenile chronic myelogenous leukemia stem cells capable of initiating the disease in primary and secondary SCID mice, Blood 88 (1996) 2655.
[8] T. Lapidot, C. Sirard, J. Vormoor, B. Murdoch, T. Hoang, J. Caceres-Cortes,

M. Minden, B. Paterson, M.A. Caligiuri, J.E. Dick, A cell initiating human acute myeloid leukaemia after transplantation into SCID mice, Nature 367 (1994) 645–648.
[9] Y. Liu, F. Chen, S. Wang, X. Guo, P. Shi, W. Wang, B. Xu, Low-dose triptolide in combination with idarubicin induces apoptosis in AML leukemic stem-like KG1a cell line by modulation of the intrinsic and extrinsic factors, Cell Death Dis. 4 (2013) e948.
[10] B. Xu, S. Wang, R. Li, K. Chen, L. He, M. Deng, V. Kannappan, J. Zha, H. Dong, W. Wang, Disulfiram/copper selectively eradicates AML leukemia stem cells *in vitro* and *in vivo* by simultaneous induction of ROS-JNK and inhibition of NF-kappaB and Nrf2, Cell Death Dis. 8 (2017) e2797.
[11] E. Yang, S.J. Korsmeyer, Molecular thanatopsis: a discourse on the BCL2 family and cell death, Blood 88 (1996) 386–401.
[12] J.M. Adams, S. Cory, The Bcl-2 Protein Family: Arbiters of Cell Survival, Science, 1998.
[13] P.E. Czabotar, L. Guillaume, S. Andreas, J.M. Adams, Control of apoptosis by the BCL-2 protein family: implications for physiology and therapy, Nat. Rev. Mol. Cell Biol. 15 (2014) 49–63.
[14] A.R. Delbridge, S. Grabow, A. Strasser, D.L. Vaux, Thirty years of BCL-2: translating cell death discoveries into novel cancer therapies, Nat. Rev. Cancer 16 (2016) 99–109.
[15] P. Luca, G. Mithat, J.R. Gardner, M. Jill, Y. Dajun, H. Jon, S. Mel, L. Lance, M. Katia, M. Guido, Targeting Bcl-2 family members with the BH3 mimetic AT-101 markedly enhances the therapeutic effects of chemotherapeutic agents in *in vitro* and *in vivo* models of B-cell lymphoma, Blood 111 (2008) 5350–5358.
[16] K. Balakrishnan, J. Burger, V. Wg, Gandhi, AT-101 induces apoptosis in CLL B cells and overcomes stromal cell-mediated Mcl-1 induction and drug resistance, Blood 113 (2009) 149.
[17] Y. Meng, W. Tang, Y. Dai, X. Wu, M. Liu, Q. Ji, M. Ji, K. Pienta, T. Lawrence, L. Xu, Natural BH3 mimetic (-)-gossypol chemosensitizes human prostate cancer via Bcl-xL inhibition accompanied by increase of Puma and Noxa, Mol. Cancer Ther. 7 (2008) 2192–2202.
[18] L. Glenn, K.W. Kevin, W. George, L. Lance, B. Kimberli, S. Bradley, An open-label, multicenter, phase I/II study of single-agent AT-101 in men with castrate-resistant prostate cancer, Clin. Cancer Res. 15 (2009) 3172–3176.
[19] H. Wenbin, W. Fang, T. Jingsheng, L. Xinyu, Y. Zhu, N. Chunlai, W. Yuquan, Proapoptotic protein Smac mediates apoptosis in cisplatin-resistant ovarian cancer cells when treated with the anti-tumor agent AT101, J. Biol. Chem. 287 (2012) 68–80.
[20] K. Burcak, A. Harika, B. Emir, K. Asli, U. Selim, K. Bülent, S. Canfeza, S. Ulus Ali, U. Ruchan, Combination of AT-101/cisplatin overcomes chemoresistance by inducing apoptosis and modulating epigenetics in human ovarian cancer cells, Mol. Biol. Rep. 40 (2013) 3925–3933.
[21] M.Q. Baggstrom, Q. Yingwei, K. Marianna, A. Athanassios, E.A. Johnson, M.J. Millward, S.C. Murphy, E. Charles, C.M. Rudin, G. Ramaswamy, A phase II study of AT-101 (Gossypol) in chemotherapy-sensitive recurrent extensive-stage small cell lung cancer, J. Thorac. Oncol. 6 (2011) 1757–1760.
[22] L. Zhang, Y. Zhou, K. Chen, P. Shi, Y. Li, M. Deng, Z. Jiang, X. Wang, P. Li, B. Xu, The pan-bcl2 inhibitor AT101 activates the intrinsic apoptotic pathway and causes DNA damage in acute myeloid leukemia stem-like cells, Target. Oncol. 12 (2017) 677–687.
[23] R. Pan, L.J. Hogdal, J.M. Benito, D. Bucci, L. Han, G. Borthakur, J. Cortes, D.J. DeAngelo, L. Debose, H. Mu, H. Dohner, V.I. Gaidzik, I. Galinsky, L.S. Golfman, T. Haferlach, K.G. Harutyunyan, J. Hu, J.D. Leverson, G. Marcucci, M. Muschen, R. Newman, E. Park, P.P. Ruvolo, V. Ruvolo, J. Ryan, S. Schindela, P. Zweidler-McKay, R.M. Stone, H. Kantarjian, M. Andreeff, M. Konopleva, A.G. Letai, Selective BCL-2 inhibition by ABT-199 causes on-target cell death in acute myeloid leukemia, Cancer Discov. 4 (2014) 362–375.
[24] T.C. Chou, Drug combination studies and their synergy quantification using the Chou-Talalay method, Cancer Res. 70 (2010) 440–446.
[25] L. Mats, Targeting the DNA damage response in cancer, Chem. Rev. 109 (2009) 2929.
[26] W.P. Roos, A.D. Thomas, B. Kaina, DNA damage and the balance between survival and death in cancer biology, Nat. Rev. Cancer 16 (2015) 20.
[27] P. Ranganathan, T. Kashyap, X. Yu, X. Meng, T.H. Lai, B. Mcneil, B. Bhatnagar, S. Shacham, M. Kauffman, A.M. Dorrance, XPO1 inhibition using selinexor synergizes with chemotherapy in acute myeloid leukemia (AML) by targeting DNA repair and restoring topoisomerase IIα to the nucleus, Clin. Cancer Res. J. Am. Assoc. Cancer Res. 22 (2016) 6142.
[28] R.A. El-Awady, M.H. Semreen, M.M. Saber-Ayad, F. Cyprian, V. Menon, T.H. Al-Tel, Modulation of DNA damage response and induction of apoptosis mediates synergism between doxorubicin and a new imidazopyridine derivative in breast and lung cancer cells, DNA Repair 37 (2016) 1–11.
[29] L.A. Mathews, S.M. Cabarcas, E.M. Hurt, Z. Xiaohu, E.M. Jaffee, W.L. Farrar, Increased expression of DNA repair genes in invasive human pancreatic cancer cells, Pancreas 40 (2011) 730.
[30] B. Shideng, W. Qiulian, R.E. Mclendon, H. Yueling, S. Qing, A.B. Hjelmeland, M.W. Dewhirst, D.D. Bigner, J.N. Rich, Glioma stem cells promote radioresistance by preferential activation of the DNA damage response, Nature 444 (2006) 756–760.
[31] J.H. Hoeijmakers, Genome maintenance mechanisms for preventing cancer, Nature 411 (2001) 366–374.
[32] W.P. Roos, B. Kaina, DNA damage-induced cell death by apoptosis, Trends Mol. Med. 12 (2006) 440–450.
[33] S. Fulda, Cell death and survival signaling in oncogenesis, Klin. Pädiatr. 222 (2010) 340–344.
[34] M. Eich, W.P. Roos, T. Nikolova, B. Kaina, Contribution of ATM and ATR to the resistance of glioblastoma and malignant melanoma cells to the methylating anticancer drug temozolomide, Mol. Cancer Ther. 12 (2013) 2529–2540.
[35] R.V. Pusapati, R.J. Rounbehler, H. Sungki, J.T. Powers, Y. Mingshan, K. Kaoru, M.J. Mcarthur, P.K. Wong, D.G. Johnson, ATM promotes apoptosis and suppresses tumorigenesis in response to Myc, Proc. Natl. Acad. Sci. U.S.A. 103 (2006) 1446–1451.
[36] H. Noriko, M. Kiyoshi, Targeting DNA damage response in cancer therapy, Cancer Sci. 105 (2014) 370–388.
[37] Y. Li, H. Wang, X. Wang, W. Jin, Y. Tan, H. Fang, S. Chen, Z. Chen, K. Wang, Genome-wide studies identify a novel interplay between AML1 and AML1/ETO in t(8;21) acute myeloid leukemia, Blood 127 (2015) 233.
[38] J. Licht, AML1 and the AML1-ETO fusion protein in the pathogenesis of t(8;21) AML, Oncogene 20 (2001) 5660.
[39] C. Ganzel, J. Becker, P.D. Mintz, H.M. Lazarus, J.M. Rowe, Hyperleukocytosis, leukostasis and leukapheresis: practice management, Blood Rev. 26 (2012) 117–122.
[40] G.J. Ventura, J.P. Hester, T.L. Smith, M.J. Keating, Acute myeloblastic leukemia with hyperleukocytosis: risk factors for early mortality in induction, Am. J. Hematol. 27 (2010) 34–37.
[41] Y. Goichi, M. Toshihiro, J.T. Siamak, I. Tadafumi, J.L. Rocnik, K. Yoshikane, M. Yasuo, S. Takahiro, I. Hiromi, T. Katsuto, FLT3-ITD up-regulates MCL-1 to promote survival of stem cells in acute myeloid leukemia via FLT3-ITD-specific STAT5 activation, Blood 114 (2009) 5034–5043.